Journal of Applied Physics

RESEARCH ARTICLE | MAY 01 2025

3ω Method for thermal conductivity measurement of thin sheet materials

Xiao Yang ; Haibo Zhao; Chunyang Wang ; Yanan Shen; Pengyu Zhang; Haisheng Chen ; Ting Zhang ; Xinghua Zheng

J. Appl. Phys. 137, 175102 (2025)
https://doi.org/10.1063/5.0251786

Journal of Applied Physics METHOD pubs.aip.org/aip/jap

3ω Method for thermal conductivity measurement of thin sheet materials

Cite as: J. Appl. Phys. **137**, 175102 (2025); doi: 10.1063/5.0251786
Submitted: 4 December 2024 · Accepted: 7 April 2025 ·
Published Online: 1 May 2025

Xiao Yang,[1,2,3] Haibo Zhao,[1,4] Chunyang Wang,[1,3] Yanan Shen,[1,4] Pengyu Zhang,[1,4] Haisheng Chen,[1,2,3,4] Ting Zhang,[1,2,3,4,5,6,a)] and Xinghua Zheng[1,3,4,a)]

AFFILIATIONS

[1]Institute of Engineering Thermophysics, Chinese Academy of Sciences, Beijing 100190, China
[2]Nanjing Institute of Future Energy System, Nanjing 211135, China
[3]Key Laboratory of Long-Duration and Large-Scale Energy Storage, Chinese Academy of Sciences, Beijing 100190, China
[4]University of Chinese Academy of Sciences, Beijing 100049, China
[5]University of Chinese Academy of Sciences, Nanjing 211135, China
[6]Innovation Academy for Light-duty Gas Turbine, Chinese Academy of Sciences, Beijing 100190, China

[a)]**Authors to whom correspondence should be addressed:** zhangting@iet.cn and zhengxh@iet.cn

ABSTRACT

The 3ω method is widely employed for measuring the thermal conductivity of bulk, powder, liquid, and fibrous materials owing to its excellent versatility and accuracy. However, for sheet materials, the 3ω method usually requires depositing a metal electrode on the material, and sheet materials with rough surfaces, therefore, are difficult to meet the testing requirements of the 3ω method. In this study, a two-dimensional heat conduction model of the 3ω method suitable for thin sheet materials with/without rough surfaces was proposed, and it was used to measure the stainless-steel sheet and aluminum foil materials. The samples were suspended by four metal testing electrodes, and their thermal conductivity was measured and compared with standard values. The results indicate that this method can accurately measure the thermal conductivity of two-dimensional thin sheet conducting materials, thus extending the practical application scope of the 3ω method.

I. INTRODUCTION

With the advancement of synthesis technologies and electronic devices, the requirements of thermal functional materials have become increasingly diverse and widespread for local thermal management and micro-/nanoscale heat transport. More adaptable and targeted materials continue to emerge at both macro- and micro-scales, such as thermoelectric materials,[1,2] thermal interface materials,[3] thermal insulation materials,[4] and phase change materials.[5] The emergence of new materials necessitates appropriate methods to characterize their physical parameters, with thermal conductivity being one of the most important parameters for functional materials utilized in the thermal management fields of electronic devices,[6,7] construction,[8] energy conversion systems,[9,10] and aerospace equipment.[11] In recent years, the characterization of thermal conductivity has advanced rapidly, with several commercial instruments available that can typically measure bulks, powders, liquids, flakes, etc., such as laser flash analyzer (LFA),[12] xenon flash analyzer (XFA),[13] hot-disk,[14] heat flow meter (HFM),[15] thermal interface material (TIM) tester,[16] and other steady-state or transient methods.[17–20] These commercially available instruments generally offer high measurement accuracy. Nevertheless, for materials such as flakes, fibers, two-dimensional (2D) films, and nanotubes, which fall within the micrometer range or smaller, meeting the measurement requirements of commercial instruments poses significant challenges. Consequently, researchers are developing laboratory methods to address the testing needs of these materials, such as the photothermal reflectance method,[21] T-type method,[22] 3ω method,[17] suspended device method,[23] Raman spectroscopy,[24] time-domain thermal reflectance method,[25] and thermal probe method.[26]

The 3ω method is distinguished from these methods, demonstrating a broad range of effectiveness from insulating to conductive materials, from solids and liquids to gases.[27–34] For thin sheet

materials, 3ω measurements are typically performed by depositing a layer of metal with a thickness of 30–300 nm on the surface of the material as a measuring electrode. This requirement necessitates a good surface roughness, which subsequently limits the application of this method.[27] In recent years, material preparation has developed rapidly, but some materials are difficult to meet the high surface roughness requirements of the 3ω method, such as thermoelectric materials, semiconductors, and heat storage materials. As a result, it is urgent to develop the 3ω method to measure the thermal conductivity of materials with rough surfaces. Table I shows the comparison with literature methods.[34–36]

In this study, the 2D transient heat conduction differential equation with an internal heat source is derived for the 3ω method applicable to thin sheet conducting materials. Then, the thermal conductivities of stainless-steel sheets and aluminum foils are calculated from experimental measurements based on the equations and compared with standard values. Given that the thickness of the sheet-like materials applicable to this method is at the micrometer scale and its thermal conductivity is considered a macroscopic value, the influence of boundary roughness is not addressed. Finally, the thermal conductivity of rough sheet conducting materials is determined, which extends the 3ω method for accurately measuring the thermal conductivity of such materials.

TABLE I. Comparison of testing methods for small-scale materials.

Measurement materials/methods	Characteristic	Reference
Rod- or filament-like specimen/3ω method	Simultaneously measure the specific heat and thermal conductivity with a high accuracy.	34
Polymer layers/3ω method	Simultaneously determine the in-plane and out-of-plane components of the thermal conductivity. Simple data analysis, convenient fabrication of devices, and high accuracy.	35
Ni thin film/self-heating microbridges with IR thermography	Determine thermal conductivity by fitting the measured temperature distribution using the finite volume method in self-heating Ni microbridges and can be applied to any metallic film without modification.	36
Thin sheet-like materials/3ω method	Suitable for both rough and smooth surfaces with self-heating technology. Simple structure and convenient measurement.	This work

II. MODELING AND DERIVATION

A measurement model was established based on the sheet material, as illustrated in Fig. 1, and the thin sheet was tested using a four-wire measurement with the 3ω method, where two wires on the sides were connected to the current and two wires in the middle were connected to the voltage. The sample distance between the two ends of the voltage is denoted as L, and the sample width is $2a$ (with the thickness of the sample being d, and $d \ll a$). The model was constructed in the x/y direction between the voltage ends. It is difficult to establish a temperature gradient in the thickness direction for thin sheet materials used in this work, and the heat conduction process in the thickness direction will not be considered. Due to the excellent heat transfer capacity of the electrode substrate, the model temperature distribution within the two voltage ends will form a parabolic distribution. Based on the 2D heat conduction equation, the transient heat conduction differential equation (1) can be formulated, incorporating the internal heat source term.

The 2D transient heat conduction differential equation is

$$\rho C_p \frac{\partial}{\partial t} T(x, y, t) - k\left(\frac{\partial^2}{\partial x^2} T(x, y, t) + \frac{\partial^2}{\partial y^2} T(x, y, t)\right) = \frac{R I_0^2 \sin^2 \omega t}{LS} [1 + \alpha(T(x, y, t) - T_0)], \quad (1)$$

$$T(0, y, t) = T_0;\ T(L, y, t) = T_0;\ T(x, -a, t) = T_0;\ T(x, a, t) = T_0;\ T(x, y, -\infty) = T_0, \quad (2)$$

where ρ, C_p, k, R, α, and S represent the density, specific heat, thermal conductivity, electric resistance, temperature coefficient of resistance, and cross section of the sample at the room temperature T_0, respectively. Assuming that the electric current is turned on at

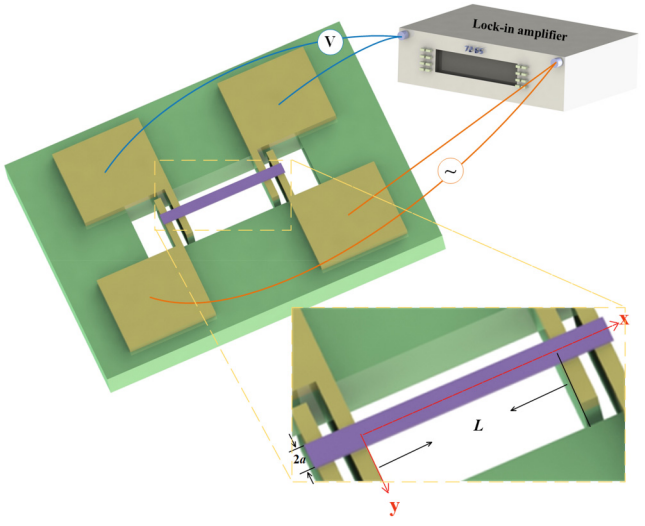

FIG. 1. Measurement model and principle.

$t = -\infty$, to simplify Eq. (1), the temperature variation is represented as the temperature difference $\Delta(x, y, t)$, with $\Delta(x, y, t) = T(x, y, t) - T_0$. Then, Eqs. (1) and (2) can be written into Eqs. (3) and (4),

$$\rho C_p \frac{\partial}{\partial t}\Delta(x, y, t) - k\left(\frac{\partial^2}{\partial x^2}\Delta(x, y, t) + \frac{\partial^2}{\partial y^2}\Delta(x, y, t)\right) = \frac{RI_0^2 \sin^2 \omega t}{LS}[1 + \alpha\Delta(x, y, t)], \tag{3}$$

$$\Delta(0, y, t) = 0;\ \Delta(L, y, t) = 0;\ \Delta(x, -a, t) = 0;\ \Delta(x, a, t) = 0;\ \Delta(x, y, -\infty) = 0. \tag{4}$$

They can also be simplified into Eqs. (5) and (6),

$$\frac{\partial}{\partial t}\Delta(x, y, t) - b\left(\frac{\partial^2}{\partial x^2}\Delta(x, y, t) + \frac{\partial^2}{\partial y^2}\Delta(x, y, t)\right) = c \sin^2 \omega t + g\Delta(x, y, t) \sin^2 \omega t, \tag{5}$$

$$b = \frac{k}{\rho C_p};\ c = \frac{RI_0^2}{LS\rho C_p};\ g = \frac{\alpha RI_0^2}{LS\rho C_p}. \tag{6}$$

According to the impulse theorem,[37] $\Delta(x, y, t)$ can be represented as the integral of the responses of the simple to the instant $c \sin^2 \omega t$ at each time interval,[27]

$$\Delta(x, y, t) = \int_{-\infty}^{t} Z(x, y, t; \tau) d\tau. \tag{7}$$

Hence, Eqs. (5) and (6) can be simplified into Eqs. (8) and (9),

$$\frac{\partial}{\partial t}Z - b\left(\frac{\partial^2}{\partial x^2}Z + \frac{\partial^2}{\partial y^2}Z\right) - Zg \sin^2 \omega t = 0, \tag{8}$$

$$Z(0, y, t) = 0;\ Z(L, y, t) = 0;\ Z(-a, t) = 0;\ Z(x, a, t) = 0;\ Z(x, y, \tau + 0) = c \sin^2 \omega\tau. \tag{9}$$

Z can be expanded through the Fourier series,

$$Z(x, y, t; \tau) = \sum_{n=1}^{\infty}\sum_{m=1}^{\infty} U_{nm}(t; \tau) \sin\frac{n\pi x}{L} \sin\frac{m\pi y}{a}. \tag{10}$$

Substituting Eq. (10) into Eq. (8) yields Eq. (11),

$$\sum_{n=1}^{\infty}\sum_{m=1}^{\infty} \sin\frac{n\pi x}{L} \sin\frac{m\pi y}{a} \times \left[\frac{dU_{nm}(t; \tau)}{dt} + U_{nm}(t; \tau)\left(\frac{L^2m^2 + a^2n^2}{\gamma} - g\sin^2\omega t\right)\right] = 0, \tag{11}$$

where $\gamma = a^2L^2/b\pi^2$ is the characteristic thermal time constant of the sample in the in-plane heat transfer. If $(L^2m^2 + a^2n^2)/\gamma$ is much larger than g, it indicates that the non-uniformity of heating power caused by resistance fluctuations along the sample should be much smaller than the total heating power. This situation is usually true (suitable sizes fall in the millimeter range). Namely,

$$\frac{dU_{nm}(t; \tau)}{dt} + U_{nm}(t; \tau)\frac{L^2m^2 + a^2n^2}{\gamma} = 0. \tag{12}$$

Therefore, the solution to Eq. (12) is

$$U_{nm}(t; \tau) = C_{nm}(\tau)e^{-\frac{L^2m^2+a^2n^2}{\gamma}(t-\tau)}. \tag{13}$$

Combining the relationship between Eqs. (8) and (9), and (14) and (15), the result of C_{nm} can be obtained,

$$\sum_{n=1}^{\infty}\frac{2[1-(-1)^n]}{n\pi}\sin\frac{n\pi x}{L} = 1,\ 0 < x < L, \tag{14}$$

$$\sum_{m=1}^{\infty}\frac{2[1-(-1)^m]}{m\pi}\sin\frac{m\pi y}{a} = 1,\ 0 < y < a, \tag{15}$$

$$C_{nm}(\tau) = c \sin^2 \omega\tau \frac{4[1-(-1)^n]}{n\pi}\frac{[1-(-1)^m]}{m\pi}. \tag{16}$$

Substituting Eq. (13) yields the relationship of $U_{nm}(t; \tau)$,

$$U_{nm}(t; \tau) = c \sin^2 \omega\tau \frac{4[1-(-1)^n]}{n\pi}\frac{[1-(-1)^m]}{m\pi}e^{-\frac{L^2m^2+a^2n^2}{\gamma}(t-\tau)}. \tag{17}$$

Substituting Eq. (10) yields the relationship of $Z(x, y, t; \tau)$,

$$Z(x, y, t; \tau) = \sum_{n=1}^{\infty}\sum_{m=1}^{\infty} c\sin^2\omega\tau \frac{4[1-(-1)^n]}{n\pi}\frac{[1-(-1)^m]}{m\pi} \times e^{-\frac{L^2m^2+a^2n^2}{\gamma}(t-\tau)} \sin\frac{n\pi x}{L}\sin\frac{m\pi y}{a}. \tag{18}$$

Substituting Eq. (7) yields the relationship of $\Delta(x, y, t)$,

$$\Delta(x, y, t) = \sum_{n=1}^{\infty}\sum_{m=1}^{\infty}\frac{2[1-(-1)^n]}{n\pi}\frac{[1-(-1)^m]}{m\pi}\sin\frac{n\pi x}{L} \times \sin\frac{m\pi y}{a}\frac{\gamma c}{(L^2m^2 + a^2n^2)}\left[1 - \frac{\sin(2\omega t + \theta)}{1 + \cot^2\theta}\right], \quad \cot\theta = 2\omega\gamma/(L^2m^2 + a^2n^2). \tag{19}$$

Temperature fluctuations can lead to resistance fluctuations, which can be described by Eq. (20),

$$\delta R = \frac{\alpha R}{aL}\int_0^a\int_0^L \Delta(x, y, t) dx dy. \tag{20}$$

According to Eq. (19), Eq.(20) can be solved as follows:

$$\delta R = \alpha R \sum_{n=1}^{\infty}\sum_{m=1}^{\infty}\left(\frac{[1-(-1)^n]}{n\pi}\right)^2\left(\frac{[1-(-1)^m]}{m\pi}\right)^2 \times \frac{2\gamma c}{(L^2m^2+a^2n^2)}\left[1-\frac{\sin(2\omega t+\theta)}{1+\cot^2\theta}\right]. \quad (21)$$

$V = I_0 \sin\omega t(R+\delta R)$ can be solved as follows:

$$V = I_0 \sin\omega t\left(R+\alpha R\sum_{n=1}^{\infty}\sum_{m=1}^{\infty}\left(\frac{[1-(-1)^n]}{n\pi}\right)^2 \times\left(\frac{[1-(-1)^m]}{m\pi}\right)^2\frac{2\gamma c}{(L^2m^2+a^2n^2)}\left[1-\frac{\sin(2\omega t+\theta)}{1+\cot^2\theta}\right]\right). \quad (22)$$

When $n = 1,\ m = 1$, the third-harmonic voltage $V_{3\omega}$ can be obtained,

$$V_{3\omega} \approx -\alpha R I_0 \frac{32}{\pi^4}\frac{\gamma c}{(L^2+a^2)}\frac{1}{1+\cot^2\theta}. \quad (23)$$

According to Eqs. (6), Eq. (23) can be simplified. Then, the relationship between thermal conductivity k and third-harmonic voltage $V_{3\omega}$ can be obtained,

$$k \approx -\frac{32\alpha R^2 I_0^3 a^2 L}{V_{3\omega} S\pi^6(L^2+a^2)}\frac{1}{1+\cot^2\theta}. \quad (24)$$

Finally, the thermal conductivity of the sample can be determined by obtaining parameters such as the temperature coefficient of resistance, resistance, first-harmonic current, length, half-width, the magnitude of third-harmonic voltage, and cross-sectional area of the material.

III. ERROR ANALYSIS

In the derivation process, two aspects were simplified, and the first was to ignore $g\sin^2\omega t$ in Eq. (11). The physical meaning of this term was expressed by the material resistance fluctuations caused by thermal disturbances, which were much smaller than the heating power. The derivation of Eq. (11) ignored the $g\sin^2\omega t$ of $(L^2m^2+a^2n^2)/\gamma - g\sin^2\omega t$. Equation (25) is the derivation of the ratio of these two terms, and the ratio of the two terms is much greater than 1 based on the test samples,

$$\begin{aligned}&\sum_{n=1}^{\infty}\sum_{m=1}^{\infty}\frac{(L^2m^2+a^2n^2)}{\gamma}/g\sin^2\omega t\\ &=\sum_{n=1}^{\infty}\sum_{m=1}^{\infty}\frac{\frac{k\pi^2}{\rho C_p}(L^2m^2+a^2n^2)}{a^2L^2}/\frac{\alpha RI_0^2}{LS\rho C_p}\sin^2\omega t\\ &=\sum_{n=1}^{\infty}\sum_{m=1}^{\infty}\frac{k\pi^2(L^2m^2+a^2n^2)S}{\alpha RI_0^2\,a^2L\sin^2\omega t}\gg 1.\end{aligned} \quad (25)$$

The second aspect was to take $n = 1,\ m = 1$ in Eq. (23) to calculate the third-harmonic voltage, ignoring the terms of $n \geq 2,\ m \geq 2$. In this case, according to the calculation, the relative error approximates 1.44%. When the lock-in amplifier output current frequency is low, $\omega\gamma \to 0$, the third-harmonic voltage is independent of the phase angle. When the output current is high, $\omega\gamma \to \infty$, ignoring the term $n \geq 2,\ m \geq 2$ will lead to a large error in the calculation of the third-harmonic voltage.

The radiant heat loss from the test sample surface was also ignored in the calculation. The radiant heat loss per unit length of the sample can be represented by the following equation:

$$Q = 2(2a+d)\varepsilon\sigma\left(T^4 - T_0^4\right), \quad (26)$$

where d denotes the sample thickness and $a,\ L \gg d$. σ is the Boltzmann constant, and ε represents the material emissivity. According to the polynomial expansion and ignoring the higher terms of $\Delta(x, y, t)$, $T^4 = 4\Delta(x, y, t)T_0^3 + T_0^4$ can be obtained, and inserting it into Eq. (26) yields the expression for the radiative heat loss,

$$Q = 8(2a+d)\varepsilon\sigma\Delta(x, y, t)T_0^3. \quad (27)$$

Substituting Q into Eq. (1) and deriving it again, the following equation needs to be satisfied to ignore the radiative heat loss,

$$\frac{L^2m^2+a^2n^2}{\gamma} \gg \frac{Q}{\Delta(x, y, t)}. \quad (28)$$

Equation (28) is simplified to the following equation:

$$\frac{8(2a+d)\varepsilon\sigma T_0^3L^2a^2\rho C_p}{k\pi^2(L^2+a^2)} \ll 1. \quad (29)$$

The uncertainty of thermal conductivity was calculated based on Eq. (24) according to the error transfer equation,[38] which included uncertainties caused by current, resistance, sample size, third-harmonic voltage, and frequency. The uncertainty equation of thermal conductivity can be expressed as follows:

$$\left(\frac{\delta k}{k}\right)^2 = 2\left(\frac{\delta R}{R}\right)^2+3\left(\frac{\delta I_0}{I_0}\right)^2+3\left(\frac{\delta a}{a}\right)^2+3\left(\frac{\delta L}{L}\right)^2 + \left(\frac{\delta d}{d}\right)^2+\left(\frac{\delta V_{3\omega}}{V_{3\omega}}\right)^2+\left(\frac{\delta\theta}{\theta}\right)^2. \quad (30)$$

The sample is connected in series with an adjustable resistor box, and the loop voltage is provided through a lock-in amplifier. The resistance of the resistor box is adjusted so that the voltage difference between the two sides of the sample and the resistance box is equal. At this point, the resistance value of the resistance box is equal to that of the sample. Then, the resistance of the samples was obtained with a minimum resistance of 1.88 ohms, a minimum resolution of 0.01 ohms, and a resistance uncertainty of 0.53%. The current was obtained by calculating the first-harmonic voltage and resistance, and the accuracy of the lock-in amplifier voltage is lower than 0.2%. Then, the uncertainty of the current was calculated to be about 0.57%. The length, width, and thickness of the sample

were determined by optical microscopy with an uncertainty of 0.5%. The uncertainty of the phase angle of third-harmonic voltage did not exceed 5%. As a result, by substituting all the uncertainties into Eq. (30), a maximum uncertainty of 5.32% was obtained for the thermal conductivity.

IV. EXPERIMENTAL STEPS

For the tests in this work, a standard stainless-steel sheet with a thickness of 10 μm and aluminum foil with a thickness of 20 μm were selected as test samples. The diagram of the test setup is illustrated in Fig. 2, where ① denotes the vacuum chamber, ② denotes the sample stage, ③ denotes the vacuum control device, and ④ denotes the signal output and detection end. The substrate carrying the sample was processed by a Printed Circuit Board (PCB), where the copper metal was deposited on a part of the surface to serve as the conductive part, and the rest of the part was suspended to minimize the effect of heat transfer of the substrate. To decrease the resistance of the contact areas, conductive silver adhesive was employed to fill the contact areas. Four copper wires were utilized to connect the copper substrate to the terminals in the test system. The lock-in amplifier system was used to input and obtain the test signals, where the voltage was input at a low frequency for measurement. The obtained first- and third-harmonic voltages, along with the phase angle and resistance values, were recorded, and the data were finally collated to calculate the thermal conductivity.

V. RESULTS AND DISCUSSION

The obtained data were calculated according to Eq. (24), and the results are shown in Fig. 3. Specifically, Figs. 3(a) and 3(b) show the verification of the data's accuracy. Based on the relationship described by Eq. (24), it is evident that the third-harmonic voltage is proportional to the cubic of the current. Hence, we performed logarithmic processing on the acquired third-harmonic voltage and current signals, and added fitting lines. The results indicate that the third-harmonic voltage and current signals of the two samples exhibit a triple relationship after logarithmic processing of the data, as shown by the

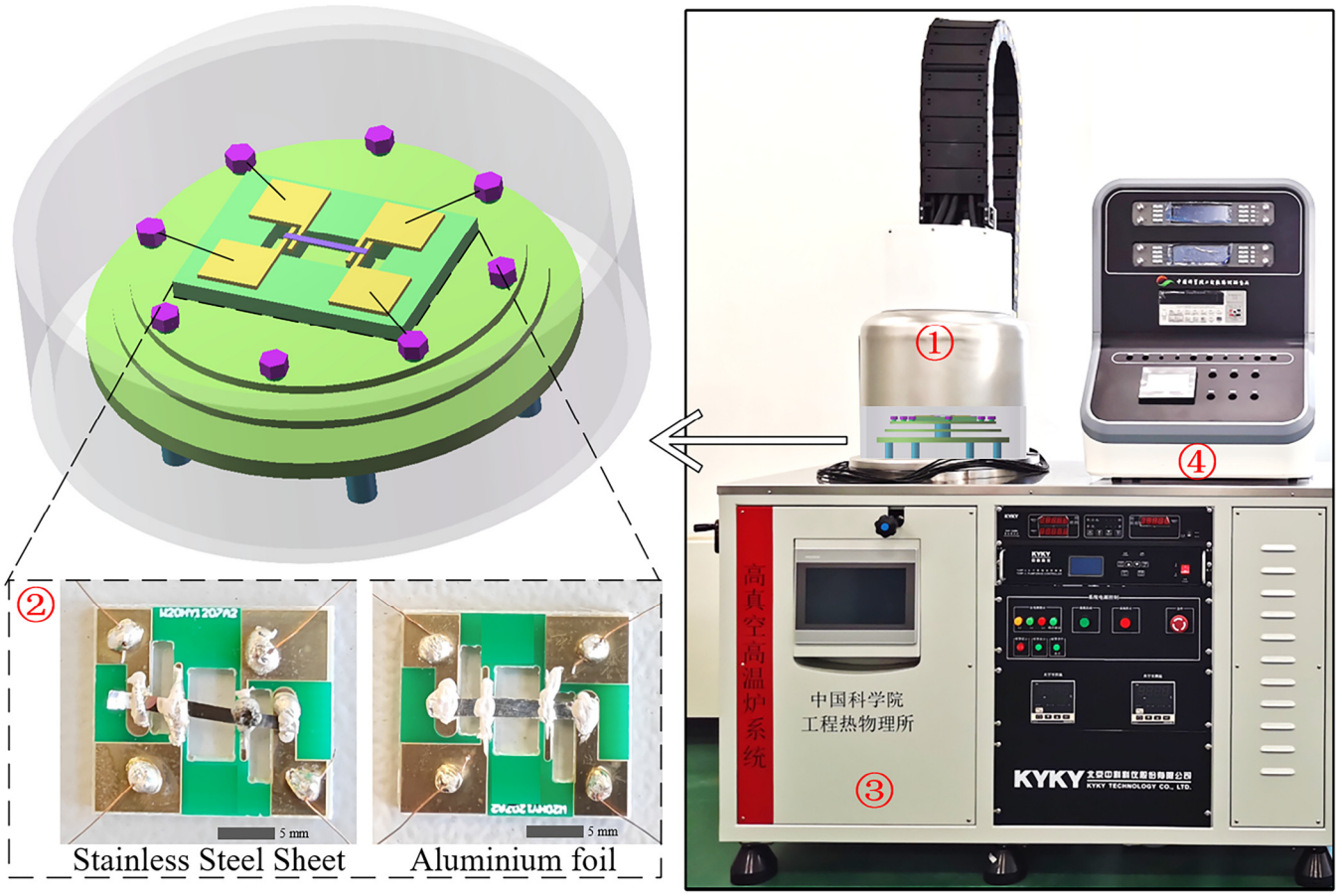

FIG. 2. Test setup and samples.

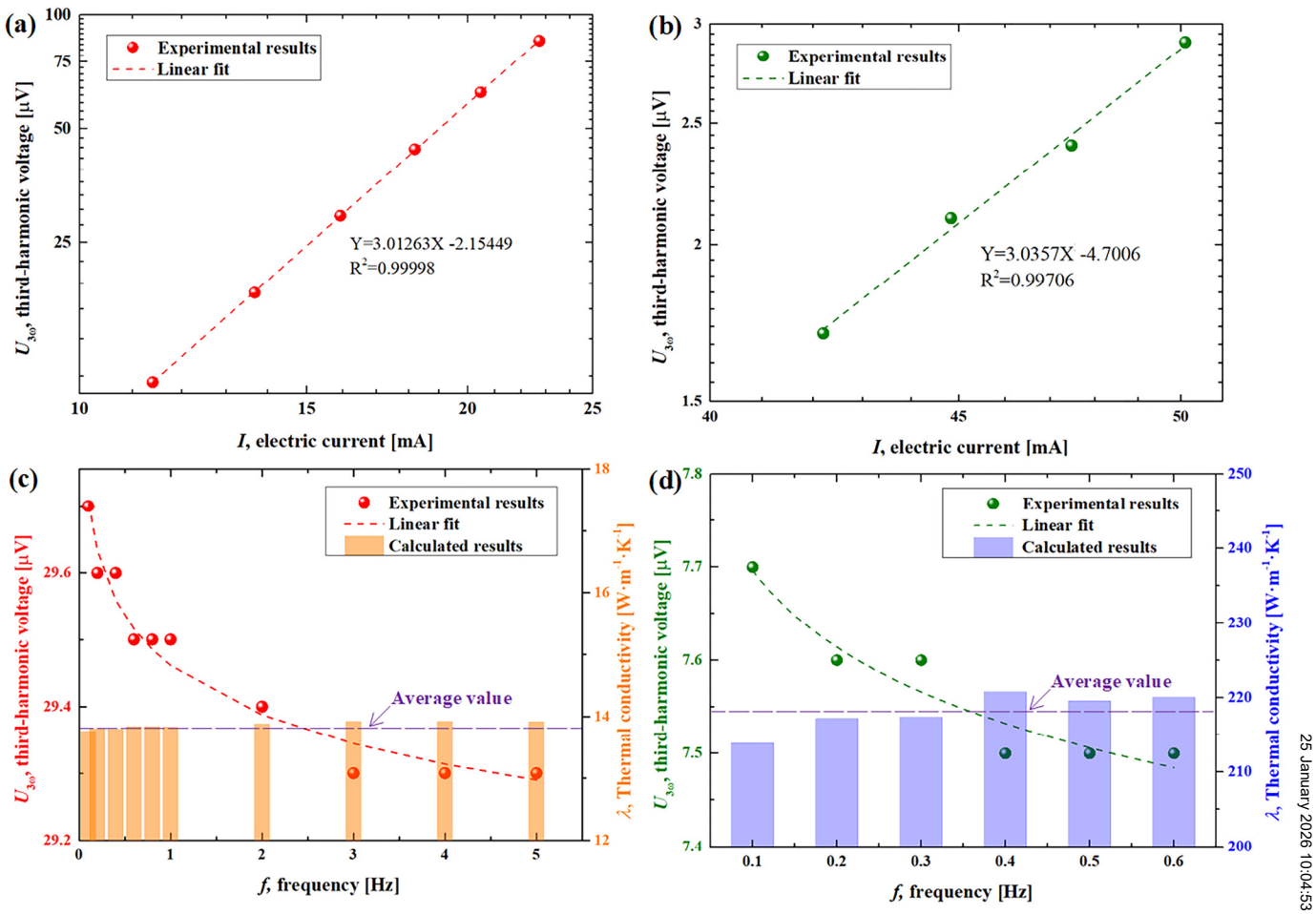

FIG. 3. Experimental results. The relationship between the third-harmonic voltage and current of stainless-steel sheet (a) and aluminum foil (b) and the relationship between the third-harmonic voltage and frequency of stainless-steel sheet (c) and aluminum foil (d).

fitting line ($Y \approx 3X$), which conforms to the logical relationship of Eq. (24) and indirectly proves that the samples are suitable for this method. Figures 3(c) and 3(d) show the relationship between the third-harmonic voltage and frequency, along with the magnitude of the calculated thermal conductivity. It can be observed from the figure that the third-harmonic voltage and frequency are inversely proportional, while the thermal conductivity values of the two samples tend to be stable. For sample 1, the average thermal conductivity is 13.85 $W\,m^{-1}\,K^{-1}$, which approximates that of stainless steel ~14 $W\,m^{-1}\,K^{-1}$.[39] For sample 2, the average value of thermal conductivity is 218.14 $W\,m^{-1}\,K^{-1}$, which is close to that of aluminum foil ~230 $W\,m^{-1}\,K^{-1}$.[39] The maximum relative uncertainties and errors of the experimental values for the two samples were 1.96% and 0.65%, and 1.07% and 5.16%, respectively. The small errors and uncertainties imply that this method can test these two types of materials effectively.

It can be found that the radiant heat loss caused by heating the samples can be ignored. According to Eq. (29), the radiant heat loss of the two samples was calculated, and the radiant heat loss coefficients of the two samples were 1.38×10^{-20} and 7.79×10^{-22}, which are much smaller than 1. The next is Eq. (11), which ignores the $g \sin^2 \omega t$ of the $(L^2m^2 + a^2n^2) / \gamma - g \sin^2 \omega t$. The calculated results indicate that the ratio $(L^2 + a^2) / \gamma g$ is much larger than 1, so the $g \sin^2 \omega t$ term can also be ignored in the derivation. Compared to more widely optical approaches, the method proposed in this work is suitable for materials with rough surfaces, which makes the 3ω method have a wider applicability.

VI. CONCLUSIONS

In this study, a 3ω method applicable to the in-plane thermal conductivity measurement of thin sheet materials was proposed, and a two-dimensional transient heat conduction differential

equation with an internal heat source term was derived. A 10 μm-thick stainless-steel sheet and a 20 μm-thick aluminum foil sheet were measured, and the average thermal conductivities were calculated to be 13.85 and 218.14 $W\,m^{-1}\,K^{-1}$, demonstrating a small testing error and high accuracy. The proposed method can effectively measure the in-plane thermal conductivity for such materials, especially those with high rough surfaces that may not be measured by other methods. The development of this method can extend the 3ω method for thin sheet materials and fill the measurement gap of these materials with rough surfaces.

ACKNOWLEDGMENTS

This work was supported by the National Key Research and Development Program of China (Grant No. 2023YFB3809800), the National Natural Science Foundation of China (NNSFC) (Grant No. 52172249), the Scientific Instrument Developing Project of the Chinese Academy of Sciences (Grant No. PTYQ2025TD0018), the Chinese Academy of Sciences Talents Program (Grant No. E2290701), the Funding of Innovation Academy for Light-duty Gas Turbine, Chinese Academy of Sciences (Grant No. CXYJJ21-ZD-02), and the Special Fund Project of Carbon Peaking Carbon Neutrality Science and Technology Innovation of Jiangsu Province (Grant No. BE2022011).

AUTHOR DECLARATIONS

Conflict of Interest

The authors have no conflicts to disclose.

Author Contributions

X.Y. and H.Z. contributed equally to this paper.

Xiao Yang: Formal analysis (equal); Methodology (equal); Writing – original draft (equal). **Haibo Zhao:** Investigation (equal); Methodology (equal). **Chunyang Wang:** Formal analysis (equal). **Yanan Shen:** Validation (equal). **Pengyu Zhang:** Validation (equal). **Haisheng Chen:** Writing – review & editing (equal). **Ting Zhang:** Funding acquisition (equal); Writing – review & editing (equal). **Xinghua Zheng:** Funding acquisition (equal); Writing – review & editing (equal).

DATA AVAILABILITY

The data that support the findings of this study are available from the corresponding authors upon reasonable request.

REFERENCES

[1]Y. Shen, C. Wang, X. Yang, J. Li, R. Lu, R. Li, L. Zhang, H. Chen, X. Zheng, and T. Zhang, "New progress on fiber-based thermoelectric materials: Performance, device structures and applications," Materials **14**, 6306 (2021).
[2]M. Tan, Y. Deng, and Y. Wang, "Ordered structure and high thermoelectric properties of $Bi_2(Te, Se)_3$ nanowire array," Nano Energy **3**, 144–151 (2014).
[3]Y. Huang, W. Luo, W. Chen, X. Hu, G. Zhu, Y. Ma, X. Jiang, and Q. Li, "Self-healing, adaptive and shape memory polymer-based thermal interface phase change materials via boron ester cross-linking," Chem. Eng. J. **496**, 153789 (2024).
[4]X. Lian, L. Tian, Z. Li, and X. Zhao, "Thermal conductivity analysis of natural fiber-derived porous thermal insulation materials," Int. J. Heat Mass Transfer **220**, 124941 (2024).
[5]X. Li, J. Wang, W. Cao, and X. Zhang, "Experimental study of temperature control based on composite phase change materials during charging and discharging of battery," J. Therm. Sci. **33**, 578–590 (2024).
[6]L. Wang, X. Li, Y. Qian, W. Li, T. Xiong, Y. Tao, Y. Li, J. Li, Y. Luo, Q. Jiang, and J. Yang, "MXene-layered double hydroxide reinforced epoxy nanocomposite with enhanced electromagnetic wave absorption, thermal conductivity, and flame retardancy in electronic packaging," Small **20**, 2304311 (2024).
[7]Y. Lin, P. Li, W. Liu, J. Chen, X. Liu, P. Jiang, and X. Huang, "Application-driven high-thermal-conductivity polymer nanocomposites," ACS Nano **18**, 3851–3870 (2024).
[8]Z. Li, W. Yang, G. Zhang, W. Ren, and Z. Shi, "Impact of thermal conductivity of aerogel-enhanced insulation materials on building energy efficiency in environments with different temperatures and humidity levels," Therm. Sci. Eng. Prog. **50**, 102540 (2024).
[9]O. Mahian, A. Kianifar, S. A. Kalogirou, I. Pop, and S. Wongwises, "A review of the applications of nanofluids in solar energy," Int. J. Heat Mass Transfer **57**, 582–594 (2013).
[10]Q. Zhang, Y. Sun, W. Xu, and D. Zhu, "Organic thermoelectric materials: Emerging green energy materials converting heat to electricity directly and efficiently," Adv. Mater. **26**, 6829–6851 (2014).
[11]G. Nobrega, B. Cardoso, R. Souza, J. Pereira, P. Pontes, S. O. Catarino, D. Pinho, R. Lima, and A. Moita, "A review of novel heat transfer materials and fluids for aerospace applications," Aerospace **11**, 275 (2024).
[12]A. Baranovskiy, A. Graff, J. Klose, J. Mayer, and Y. Amouyal, "On the origin of vibrational properties of calcium manganate based thermoelectric compounds," Nano Energy **47**, 451–462 (2018).
[13]R. Zare, H. Sharifi, M. R. Saeri, and M. Tayebi, "Investigating the effect of SiC particles on the physical and thermal properties of Al6061/SiCp composite," J. Alloys Compd. **801**, 520–528 (2019).
[14]V. Goyal, D. Teweldebrhan, and A. A. Balandin, "Mechanically-exfoliated stacks of thin films of Bi_2Te_3 topological insulators with enhanced thermoelectric performance," Appl. Phys. Lett. **97**, 133117 (2010).
[15]A. Hoseini, A. Malekian, and M. Bahrami, "Deformation and thermal resistance study of aerogel blanket insulation material under uniaxial compression," Energy and Buildings **130**, 228–237 (2016).
[16]Y. Zheng, *Interfacial Thermal Resistance Measurements of Solution Deposited CNT Films on Copper Substrates* (Auburn University, Alabama, 2015).
[17]D. G. Cahill, "Thermal conductivity measurement from 30 to 750 k: The 3ω method," Rev. Sci. Instrum. **61**, 802–808 (1990).
[18]D. Kraemer and G. Chen, "A simple differential steady-state method to measure the thermal conductivity of solid bulk materials with high accuracy," Rev. Sci. Instrum. **85**, 025108 (2014).
[19]X. Yang, C. Wang, R. Lu, Y. Shen, H. Zhao, J. Li, R. Li, L. Zhang, H. Chen, T. Zhang, and X. Zheng, "Progress in measurement of thermoelectric properties of micro/nano thermoelectric materials: A critical review," Nano Energy **101**, 107553 (2022).
[20]L. Qiu, N. Zhu, Y. Feng, E. Michaelides, G. Żyła, D. Jing, X. Zhang, P. Norris, C. Markides, and O. Mahian, "A review of recent advances in thermophysical properties at the nanoscale: From solid state to colloids," Phys. Rep. **843**, 1–81 (2020).
[21]O. W. Käding, H. Skurk, and K. E. Goodson, "Thermal conduction in metallized silicon-dioxide layers on silicon," Appl. Phys. Lett. **65**, 1629–1631 (1994).
[22]X. Zhang, S. Fujiwara, and M. Fujii, "Measurements of thermal conductivity and electrical conductivity of a single carbon fiber," Int. J. Thermophys. **21**, 965–980 (2000).
[23]P. Kim, L. Shi, A. Majumdar, and P. L. Mceuen, "Thermal transport measurements of individual multiwalled nanotubes," Phys. Rev. Lett. **87**, 215502 (2001).
[24]A. A. Balandin, S. Ghosh, W. Bao, I. Calizo, D. Teweldebrhan, F. Miao, and C. N. Lau, "Superior thermal conductivity of single-layer graphene," Nano Lett. **8**, 902–907 (2008).

[25]J. Zhu, D. Tang, W. Wang, J. Liu, K. W. Holub, and R. Yang, "Ultrafast thermoreflectance techniques for measuring thermal conductivity and interface thermal conductance of thin films," J. Appl. Phys. **108**, 094315 (2010).
[26]W. Chen, Y. Feng, L. Qiu, and X. Zhang, "Scanning thermal microscopy method for thermal conductivity measurement of a single SiO_2 nanoparticle," Int. J. Heat Mass Transfer **154**, 119750 (2020).
[27]D. G. Cahill and R. O. Pohl, "Thermal conductivity of amorphous solids above the plateau," Phys. Rev. B **35**, 4067–4073 (1987).
[28]D. G. Cahill, M. Katiyar, and J. R. Abelson, "Thermal conductivity of a-Si: H thin films," Phys. Rev. B **50**, 6077–6081 (1994).
[29]L. Qiu, X. H. Zheng, J. Zhu, G. P. Su, and D. W. Tang, "The effect of grain size on the lattice thermal conductivity of an individual polyacrylonitrile-based carbon fiber," Carbon **51**, 265–273 (2013).
[30]L. Qiu, X. Wang, D. Tang, X. Zheng, P. M. Norris, D. Wen, J. Zhao, X. Zhang, and Q. Li, "Functionalization and densification of inter-bundle interfaces for improvement in electrical and thermal transport of carbon nanotube fibers," Carbon **105**, 248–259 (2016).
[31]L. Qiu, X. Wang, G. Su, D. Tang, X. Zheng, J. Zhu, Z. Wang, P. M. Norris, P. D. Bradford, and Y. Zhu, "Remarkably enhanced thermal transport based on a flexible horizontally-aligned carbon nanotube array film," Sci. Rep. **6**, 21014 (2016).
[32]L. Qiu, X. H. Zheng, J. Zhu, D. W. Tang, S. Y. Yang, A. J. Hu, L. L. Wang, and S. S. Li, "Thermal transport in high-strength polymethacrylimide (PMI) foam insulations," Int. J. Thermophys. **36**, 2523–2534 (2015).
[33]X. Zheng, L. Qiu, G. Su, D. Tang, Y. Liao, and Y. Chen, "Thermal conductivity and thermal diffusivity of SiO_2 nanopowder," J. Nanopart. Res. **13**, 6887–6893 (2011).
[34]L. Lu, W. Yi, and D. L. Zhang, "3ωmethod for specific heat and thermal conductivity measurements," Rev. Sci. Instrum. **72**, 2996–3003 (2001).
[35]K. Kurabayashi, M. Asheghi, M. Touzelbaev, and K. E. Goodson, "Measurement of the thermal conductivity anisotropy in polyimide films," J. Microelectromech. Syst. **8**, 180–191 (1999).
[36]R. A. Sayer, J. Zeng, H. H. Hsu, D. Peroulis, and T. S. Fisher, "Thermal and electrical conductivities of nanocrystalline nickel microbridges," J. Microelectromech. Syst. **21**, 850–858 (2012).
[37]J. Zabczyk, *Mathematical Control Theory: An Introduction* (Birkhäuser, Boston, 1992).
[38]J. R. Taylor and W. Thompson, "An introduction to error analysis: The study of uncertainties in physical measurements," Phys. Today **51**, 57–58 (1998).
[39]X. Zheng, P. Yue, S. Li, L. Wang, X. Yang, and H. Chen, "Stethoscope-type 3 ω independent detector for fast measurement of material thermal conductivity," Rev. Sci. Instrum. **89**, 084904 (2018).